MicroRNAs 7/17/155 As A Potential Breast Tumor Stemness miRNA Cluster: Detection of Breast Cancer Grade Specific miRNA-mRNA Interaction Network Inspiration from Mammary Gland Development

Saeed Khodayari (saeed.khodayari@hotmail.com)
Tehran University of Medical Sciences Children's Hospital https://orcid.org/0000-0002-7831-8006
Hamid Khodayari
TUMS: Tehran University of Medical Sciences
Haniyeh Jallali
Kharazmi University
Elnaz Saeedi
University of Leicester
Ali Faryabi
TUMS: Tehran University of Medical Sciences
Meghdad Yeganeh
Royan Institute for Stem Cell Biology and Technology
Ahad Mohammadnejad
TUMS: Tehran University of Medical Sciences
Amirnader Emami Razavi
TUMS: Tehran University of Medical Sciences
Mohammad Dashtkoohi
TUMS: Tehran University of Medical Sciences
Farimah Hadjilooei
TUMS: Tehran University of Medical Sciences
Reza Shirkoohi
TUMS: Tehran University of Medical Sciences
Ramesh Omranipour
TUMS: Tehran University of Medical Sciences
Karim Nayernia
University of Gottingen: Georg-August-Universitat Gottingen
Habibollah Mahmoodzadeh
TUMS: Tehran University of Medical Sciences

Research Article

Keywords: Breast cancer, MicroRNAs 7/17/155, Breast tumor stemness, In silico analysis, Transcriptional validation, Breast cancer grade, miRNA-mRNA interaction, Mammary gland development

Posted Date: October 17th, 2022

DOI: https://doi.org/10.21203/rs.3.rs-2125843/v1

Abstract

Background

The process of breast tumor dedifferentiation is complex and unclear. The mechanism represents the origin of the genesis and development of high-grade breast stem cells. It seems that microRNAs have crucial regulatory functions in this complicated phenomenon. The main objective of this study is to identify a potential "breast tumor stemness miRNA cluster" using an in silico strategy and qRT-PCR validation guided by the molecular pattern of mammary gland development (MGD).

Methods

Microarray databases GEO and ArrayExpress were used to determine mRNA and microRNA expression in different grades of breast carcinoma (BC). Differential gene expression of mRNA (GSE29044) and miRNA (GSE4566) in three grades of BC was analyzed using GEO2R compared with normal tissue. The enrichment results revealed MGD -associated mechanisms and target mRNAs. Using the BC database, the interaction between target mRNAs and significantly altered miRNAs ($PV \leq 0.05$) in each BC grade was found by miRNet. After confirming our results using the GSE26659 data, the expression of the target miRNAs in tissue samples (24 BC, 17 normal tissues) was examined by real-time PCR. miRwalk and the STRING database discovered the miRNAs of interest and mRNA networks.

Results

The MGD stages of puberty, pregnancy and lactation, and mammary gland epithelial development were significantly involved in the upregulated genes of GI and GII tumors. No significant upregulated MGD mechanisms were detected in GIII BC. In silico analysis revealed that miRs 7/17/155 had an upregulation pattern and miR-26a had a downregulation pattern. qPCR showed that the miRNAs 7/17/155 were significantly upregulated in GIII tumors ($PV \leq 0.05$), while there were no notable changes in miR-26a. EGFR was the central node regulated by the miR 7/17/155 intermediate mRNA cluster.

Conclusions

Our results suggest that microRNAs 7/17/155 may be a potential cluster associated with formation of breast tumor stemness. This cluster can be used for the breast cancer dedifferentiation therapy or molecular classification of mammary tumor differentiation status.

Background

Mammary glands (MG) are specialized organs for milk production during lactation or breastfeeding. This gland is structured by ductal and lobular networks covered by luminal epithelium [1, 2]. In females, the

development of the MG is divided into four discrete stages, including I) embryonic phase, II) puberty, III) pregnancy-lactation, and IV) involution [1–3]. Evidence suggests that changes in the expression pattern of paracrine and growth factors initiate the transition to each MGD stage [1, 3]. Following pre-puberty development, estrogen hormone in conjunction with epidermal growth factor (EGF) causes ductal elongations to form terminal buds. During maturation, the hormone progesterone and insulin-like growth factor 1/2 (IGF 1/2) generate an extensive lateral branching of ducts [4]. The production of the prolactin during the pregnancy and oxytocin during lactation induce the GATA binding protein 3 (GATA3), signal transducer and activator of transcription 5A (STAT5A), and CCAAT/enhancer-binding protein β (C/EBPβ) signaling pathways on the epithelium of the MG. This cascade promotes alveologenesis and lactation differentiation [3, 5]. Finally, IGFBP5 and transforming growth factor β3 (TGF-β3) lead to degeneration of the lateral alveolus at the stage of involution [1, 4].

Breast carcinoma (BC) is a malignant mass in the MG epithelium that includes most malignancies of the breast [6]. Breast cancer cells (BCCs) have an abnormal phenotype depending on the similarity to their cellular origin; they are classified into three grades. Grade I (GI) or well-differentiated malignant cells that appear more like normal epithelial cells, grade II (GII) cell is a moderately differentiated carcinoma cell, and grade III (GIII) cell also refers to an undifferentiated or stem tumor cell with abnormal morphology [7]. GIII BCCs have increased proliferation and migration potential, which is considered a challenge in the treatment of patients with BC [7, 8].

The process of formation and development of high-grade breast tumor stem cells is one of the most important research questions. Inspirating developmental mechanisms seem to be a reasonable approach to interpret the origin of these cells [9]. On this basis, epithelial to mesenchymal transition (EMT) is an acceptable theory. The EMT states that stimulation of well-differentiated BCCs by some factors, mainly TGF-β, fibroblast growth factor (FGF), epidermal growth factor (EGF), and also bone morphogenetic proteins (BMPs) leads to conversion to an undifferentiated mesenchymal phenotype [10]. Although the EMT theory describes the origin of stem tumor cells with a mesenchymal phenotype, this model cannot clarify the origin of nonmesenchymal undifferentiated BCCs because they show heterogeneous molecular characteristics [11]. Using the molecular pattern of MGD may be a practical approach to find a mechanism involved in the BCCs upgrading.

MicroRNAs (miRNAs) are noncoding small single-stranded RNAs that play regulatory roles in biological mechanisms as well as in the MGD and breast carcinogenesis [12–15]. Damavandi et al. (2016) observed that the expression levels of miRNAs associated with breast development, miR-212/miR-132 family, were significantly reduced in high-grade breast tumors [16]. Despite the information from this study, detailed investigations need to obtain miRNA clusters associated with MGD in the generating high-grade BCCs. Therefore, the main objective of this study is to discover miRNA clusters for breast tumor stemness miRNA cluster by detecting miRNA-mRNA interaction networks active in different tumor grades inspired by MGD molecular mechanisms.

Methods

Microarray Datasets Collection

Microarray databases Gene Expression Omnibus database (GEO, http://www.ncbi.nlm.nih.gov/geo) and ArrayExpress (https://www.ebi.ac.uk/arrayexpress/experiments/browse.html) were used to determine mRNA and microRNA expression at different grades of BC (Fig. 1). The mRNA microarray data of GSE29044 were selected and generated using an Affymetrix Human Genome U133 Plus 2.0 Array (GPL570). A total of 102 breast samples, including 32 normal samples, 3 GI BC, 36 GII BC, and 26 GIII BC, were collected from this dataset. The miRNA microarray data from GSE45666 were used for differential miRNA expression analysis. A total of 75 breast samples, including 11 normal samples, 8 GI BC, 26 GII BC, and 30 GIII BC, were collected from this data set (Fig. 1).

Identification Of Differentially Expressed Mirnas And Mrnas

GEO2R online software was used to identify differential gene expression (DEGs) and differential miRNA expression (DEMs) between GI, GII, and GII BCs and normal tissue. Considering the P-value ≤ 0.05, upregulated (positive LogFc) and downregulated (negative LogFc) miRNAs and mRNAs were identified between GI tumor- normal tissue, GII tumor- normal tissue, and GIII tumor- normal tissue (Fig. 1). Volcano plots were generated using VolcaNoSer software (https://goedhart.shinyapps.io/VolcaNoseR) to visualize significant DEMs and DEGs. In addition, jvenn software (http://www.bioinformatics.com.cn/static/others/jvenn) was used for Venn analysis to detect the significant DEMS and DEGs.

Pathway And Gene Set Enrichment Analysis

The EnrichR tool (https://maayanlab.cloud/Enrichr) was used to analyze the enrichment of KEGG pathways, WIKI pathways, and Gene Ontology (GO) of the GI, GII, and GIII BC specific up and down-regulated DEGs. The five most significant pathways in each category were visualized using -Log10Pv and odds ratio. DIANA-miRPath v3 tool (https://dianalab.e-ce.uth.gr/html/mirpathv3/index.php?r=mirpath) was also used to the enrichment of KEGG pathways for the three BC grade-specific upregulated and downregulated DEMs. The five interesting pathways of each category were visualized using -Log10Pv. For pathway enrichment analysis of the target miRNAs, miRWALK software (http://mirwalk.umm.uni-heidelberg.de/search_mirnas) was used. Enrichment results for KEGG pathways and biological processes were visualized by SRplot (https://www.bioinformatics.com.cn) (Fig. 1).

Detecting Involved Mgd Mechanisms And Target Mrna

Results from the WIKI pathway and biological process enrichment in significantly upregulated and downregulated DEGs (PV ≤ 0.05) were used to mine MGD stages and their target mRNAs in the GI, GII, and GIII BCs. MGD stages such as embryonic development (WP2813), puberty (WP2814), pregnancy and lactation (WP2817), and involution (WP2815) were our targets in the WIKI pathway enrichment.

Mammary gland development (GO:0030879), mammary gland epithelial development (GO:0061180), mammary gland epithelial cell differentiation (GO:0060644), and regulation of mammary gland epithelial cell proliferation (GO:0033599) were also the other mechanisms of interest in the GO biological process enrichment (Fig. 1). Sankey diagrams of the discovered active and repressed MGD mechanisms in the GI, GII, and GIII BC were generated using SankeyMATIC tool (https://sankeymatic.com). Heat maps were also created to visualize target mRNA expression using SRplot on the results of GSE29044 gene expression analysis for the three different grades.

Mirna-mrna Integrated Analysis

The breast carcinoma platform of miRNet 2.0 (https://www.mirnet.ca/miRNet/home.xhtml) was used to detect and visualize the miRNA-mRNA interaction network between each BC grade's target upregulated mRNAs with significantly ($PV \leq 0.05$) upregulated DEMs (Fig. 1).

Target Mirnas Expression Validation

We used the normalized expression value (Log2) of the GSE26659 samples to validate the expression of the target miRNAs. 85 breast samples from this observation, including 18 normal samples, 4 GI BC, 32 GII BC, and 31 GIII BC, were collected for this analysis. RStudio software with the ggplot2 package was used to generate boxplots to the miRNA expression values.

Tissue Sample Preparation And Ethics

Twenty-four new female BC cases (age 32–65) with approved breast malignancy were registered in this study. Before biopsy, all patients gave written informed consent. Biopsies were obtained using ultrasound-guided 14-gage core needle biopsies with pro-mag ultra-automatic biopsy instruments. Samples were immediately transferred to sterile DNase / RNase -free cryotubes and stored in liquid nitrogen. The tissue samples were 4 GI, 10 GII, 10 GIII tumors, and 15 normal tissues. Tumor grades were determined by a blinded pathologist using hematoxylin and eosin (H&E) staining according to the Nottingham grading system. All the process were performed between February and March 2022 at the Cancer Institute of Iran, Tehran University of Medical Sciences (ethical code: IR.TUMS.IKHC.REC.1400.506).

Quantitative Real-time Pcr (Qrt-pcr)

According to the manufacturer's instructions, total RNA was extracted from the 50 g homogenized tissues using a miRNA isolation kit (Favorgen, Taiwan). Approximately 10 µl of total RNA for cDNA synthesis was reverse transcribed using BONmiR 1st-strand cDNA synthesis kit according to the manufacturer's recommendations (Bonyakhteh, Tehran, Iran) in a 20 µl reaction mix. The qRT-PCR was performed using

SYBR Green qPCR Master Mix (Invitrogen Life Technologies) on an ABI Prism 7900HT system in triplicate. We used miRNA16 as housekeeping and normalized expression using the standard comparative method CT (*ΔΔCT*). Boxplots for miRNA expression in four groups were generated using RStudio software and the ggplot2 package. The miRNA-specific RT stem-loop and forward primer sequence are shown in Table 1.

Target Mirnas Interaction Network And Ppi Network Construction

The miRWalk database with a score of > 0.95 was used to isolate the target mRNAs of the discovered miRNAs and their interaction network. We used the STRING database to detect the common miRNA-protein-protein interaction (PPI) network. The PPI network was visualized using Cytoscape software V 3.8.0 (Fig. 1).

Statistical analysis

Data were presented as mean ± standard deviation and analyzed using SPSS 26.0 software (IBM, USA). ANOVA test was performed for comparing the mean between the groups, and also Tukey test was used as a posthoc test in our analysis. We consider α = 0.05 as the lowest significant level for the analysis.

Result

DEGs and grade-specific mRNAs enrichment analysis

DEGs analysis shows differences in the mRNA expression patterns between GI, GII, and GIII BC compared with normal breast tissue (Fig. 2; A). The volcano plot and Venn diagram of significantly upregulated and downregulated DEGs displayed that with increasing tumor grade, the variation and expression level of mRNAs increased significantly (Fig. 2; A and B). 779 mRNAs in GI and 575 mRNAs in GII tumors were specifically upregulated; 1350 mRNAs were specifically upregulated in GIII tumors. Conversely, 274 mRNAs were specifically downregulated in GI and 621 mRNAs were specifically downregulated in GII tumors; in addition, 1234 mRNAs were downregulated exclusively in GIII tumors (Fig. 2; B).

Overrepresentation analysis using KEGG pathway terms of the 779 GI tumor upregulated DEGs, basal transcription (PV = 0.008), MAPK signaling (PV = 0.04), and arrhythmogenic right ventricular cardiomyopathy (PV = 0.079) were identified as the major pathways associated with this gene list. Analysis of the 272 GI tumor downregulated mRNAs also showed that Parkinson disease (PV = 0.002), non-alcoholic fatty liver disease (PV = 0.006), and apoptosis (0.014) were the most suppressed pathways (Fig. 2; C). The KEGG enrichment results of GII tumor DEGs showed that herpes simplex virus 1 infection (PV = 0.0), inositol phosphate metabolism (PV = 0.018), and endocytosis (PV = 0.031) were the major mechanisms with the 575 upregulated mRNAs. The PPAR signaling pathway (PV = 0.002), viral protein interaction with cytokine and cytokine receptor (PV = 0.004), and p53 signaling pathway (PV = 0.007) were also the major signaling pathways associated with the 621 downregulated mRNAs in the GII tumor

(Fig. 2; D). Analysis of the 1350 upregulated DEGs in GII tumor showed that primary immunodeficiency (PV = 4.44E-06), Th17 cell differentiation (PV = 8.14E-06), and human T-cell leukemia virus 1 infection (PV = 2.97E-05) were significantly interested. Among the 1234 downregulated DEGs, the pathways of herpes simplex virus 1 infection (PV = 4.11E-12), TGF-β signaling pathway (PV = 6.07E-04), and pathways in cancer (PV = 0.005) were the most affected (Fig. 2; E).

Detection Of Mgd Mechanisms In Different Grades Of Bc And Their Ppi

Investigating the results of the WIKI pathways and biological processes GO analysis of the significantly up- and down-regulated DEGs of GI, GII, and GIII tumors showed that the MGD process was strongly engaged in the lower grade breast tumors (GI and GII) (Fig. 6). Our analysis also revealed that by the BC upgrading, the patterns of MGD were diluted. Based on the WIKI pathway enrichment, the MGD stages of puberty (PV = 0.019) and pregnancy and lactation (PV = 0.034) were significantly associated with GI tumor upregulated DEGs, whereas the MGD stages of embryonic development (PV = 0.016) and pregnancy and lactation (PV = 0.017) were significantly related with GI tumor downregulated DEGs (Fig. 6; A and B). In the GII tumor, puberty (PV = 0.034) and pregnancy and lactation (PV = 0.011) were significantly associated with upregulated DEGs. The stages of embryonic development (PV = 0.016) and pregnancy and lactation (PV = 0.017) were significantly related with DEGs downregulated in the GII tumor (Fig. 6; A and B). In the GIII tumor, only pregnancy and lactation stage were significantly downregulated by MGD (PV = 0.028) (Fig. 3; A and B).

Overrepresentation analysis with GO biological process collection on the GI tumor upregulated DEGs, mammary gland epithelium development (0.02), mammary gland epithelial cell differentiation (0.04), and mammary gland development mechanism (0.041) were significantly followed up. However, no significant MGD mechanism was found in the GI tumor downregulated DEGs (Fig. 6; A and B). In the GII tumor, only mammary gland epithelium development (0.034) was detected in the upregulated gene lists, whereas no practical linkage was found in the downregulated DEGs (Fig. 6; A and B). Mammary gland development (PV = 0.016) was the only significant GIII tumor MGD mechanism based on the biological GO analysis in the downregulated genes (Fig. 6; A and B).

The expression change (LogFc) of the detected mRNAs was visualized in the three grades of BC. Venn analysis of the 49 target mRNAs revealed 5 specific genes in the GI (VEGFA, TGFB3, AREG, NRG1, and WNT7B), 7 in the GII tumor (PTPN1, USF2, ATP2C2, TTC9, TIMP1, ID2, and ERBB2), and 7 in the GIII tumor (TNFSF11, CSN3, CELF4, GLI2, NOTCH4, OXTR, and CELF5) (Fig. 6; C). The PPI analysis of the 49 mRNAs shows that GI and GII tumors specific mRNAs play a central role in this network (Fig. 6; D). The miRNAs ESR1 (33 edge count), AKT1 (31 edge count), MYC (30 edge count), ERBB2 (27 edge count), EGFR (26 edge count), CCND1 (26 edge count), and PGR (22 edge count) were the hub genes with higher interaction degree (Fig. 6; D). The GI tumor-specific mRNAs AREG and TIMP1 were the other hubs with the highest

degree of interaction in this PPI network, with 13 and 11 edge values, respectively. The mRNAs TP2C2 from the GII and CELF4/ CELF5 from the GIII tumors were not involved in this network (Fig. 6; D).

Dems And Grade-specific Mirnas Enrichment Analysis

The results of DEMs analysis show that miRNA expression patterns are different between the GI, GII, and GIII BC compared with normal breast tissue (Fig. 3; A). The volcano plot and Venn diagram showed that the divergence and level of miRNA expression were more pronounced in the downregulated DEMs in all three BC grades (Fig. 3; A and B). 10 miRNAs in the GI, 6 miRNAs in the GII, and 20 miRNAs in the GIII tumors were specifically upregulated. In turn, 56 miRNAs in GI, 55 miRNAs in GII, and 12 miRNAs in GIII tumors were specifically downregulated (Fig. 4; B).

KEGG enrichment analysis of the 10 GI tumors upregulated miRNAs showed that ECM-receptor interaction (PV = 4.55E-59), amoebiasis (PV = 2.79E-05), and glioma (PV = 8.46E-05) were the pathways most strongly associated with this gene list. Morphine addiction (PV = 1.58E-10), proteoglycans in cancer (PV = 2.94E-09), and pathways in cancer (PV = 1.93E-08) were the most involved mechanisms associated with the 56 GI tumor downregulated DEMs (Fig. 4; C). Analysis of the GII tumor DEMs showed that ErbB signaling pathway (PV = 0.002), proteoglycans in cancer (PV = 0.004), and glioma (PV = 0.004) were the three most significant cascades associated with the 6 upregulated miRNAs. In contrast, the Hippo pathway (PV = 2.14E-08), proteoglycans in cancer (PV = 2.65E-08), and ErbB signaling pathway (PV = 4.05E-07) were the major signaling pathways associated with the 55 downregulated miRNAs in the GII tumor (Fig. 4; D). In addition, analysis of the 20 GIII tumors that had upregulated DGMs showed glioma (PV = 4.99E-09), proteoglycans in cancer (PV = 6.15E-08), and ErbB signaling pathway (PV = 1.55E-07) were significantly activated. Among the 12 miRNAs downregulated by GIII tumor, ECM-receptor interaction (PV = 0.0016), PI3K-Akt signaling pathway (PV = 0.0024), and signaling pathways regulating pluripotency of stem cells (PV = 0.0024) were the most downregulated (Fig. 4; D).

Mirna-mrna Interaction Network, Candidate Mirnas Selection, And Enrichment Analysis

miRNA-mRNA interaction network, candidate miRNAs selection, and enrichment analysis
A relatively different miRNA-mRNA interaction pattern was found in the GI, GII, and GIII tumors MGD mRNAs with significantly altered expressed miRNAs (Fig. 5; A). The GI tumor exhibited a more complex miRNA-mRNA interaction network with more interacting nodes. There were 22 miRNAs involved in the GI tumor-specific miRNA-mRNA network, which hsa-miR-17-5p, hsa-miR-20a-5p, hsa-miR-20b-5p, and hsa-miR-106-5p found as hub miRNAs. Vascular endothelial growth factor A (VEGFA) was also the most involved mRNA in the GI tumor-specific interaction network (Fig. 5; A). The GII tumor miRNA-mRNA interaction network had the lowest degree of interaction. Only 7 potential miRNAs, including hsa-let-7b-5p, hsa-miR-15a-5p, hsa-miR-16a-5p, hsa-miR-20a-5p, hsa-miR-21-5p, hsa-miR-26a-5p, and also hsa-miR-106b-5p, were detected as hub miRNAs. TP53, CCND1 and MYC were also observed as primary MGD

mRNA in the miRNA-mRNA network of GII tumor (Fig. 5; A). In the GIII tumor, 23 miRNAs with high interaction were detected. hsa-miR-20a-5p, hsa-miR-17-5p, hsa-miR-16-5p and hsa-miR-106b-5p interacted most frequently. Other microRNAs such as hsa-miR-19a-3p, hsa-miR-19b-3p, hsa-miR-15b-5p, and also hsa-let-7b-5p were involved with a lower degree of interaction. NB3C1, PTEN, MYC, YY1, and KPNA6 mRNAs were found to be the major MGD mRNAs of GIII tumor (Fig. 5; A).

Following the miRNA-mRNA interaction analysis, a total of 25 miRNAs were selected as targets of interest (Fig. 5; B). The heatmap results for miRNA expression in GI, GII and GIII tumors from the GSE45666 DEMs showed that 11 microRNAs had an optimistic expression pattern. miR-7, miR-17, miR-19a, miR-19b, miR-20b, miR-24, mir-27a and miR-155 were the candidates with the gain-of-function expression pattern. In contrast, let-7b, let-7e, and miR-26a were the candidates with the loss-of-function expression pattern (Fig. 5; B). The enrichment analysis of the 11 candidate miRNAs on KEGG pathways showed that axon guidance (PV = 0.002), endocytosis (PV = 0.012), proteoglycans in cancer (PV = 0.02), GABAergic synapse (PV = 0.023), and TGF-β signaling pathway (PV = 0.025) were the major pathways regulated by this miRNA set (Fig. 5; C). In addition, these miRNAs were involved in the positive regulation of transcription, DNA-templated (PV = 0.0003), nervous system development (PV = 0.0005), protein ubiquitination (PV = 0.0005), intracellular signal transduction (0.0017), and ubiquitin-dependent protein catabolic process (PV = 0.002), based on enrichment analysis results for biological processes (Fig. 5; C).

Candidate Mirnas Expression Confirmation And Target Mirnas Selection

The expression pattern of the candidate miRNAs was examined using the data (fold change) of the GSE26659 samples to select the target miRNAs (Fig. 6). This observation revealed a relatively similar pattern to the heat map result (Fig. 5; B). Compared with the normal and GI tumor samples, the level of microRNAs let-7b/ let-7e/ miR-7/ miR-17/ miR-20b/ miR-27a/ miR-155 showed an increasing pattern in the GII and GIII BCs (Fig. 6). The microRNAs miR-19a/ miR-19b/ miR-24/ miR-26a also decreased in GII or GIII tumors compared with normal and GI tumor samples (Fig. 6). According to the grade-dependent harmony, miR-7/miR-17/miR-26a/ miR-155 were selected as target miRNAs for breast tumor stemness miRNAs (Fig. 6).

Qrt-pcr Result, Detected Mirnas Enrichment Analysis, And Network Analysis

The results of qRT-PCR for the target miRNAs showed that the expression of miR-7, miR-17, and miR-155 was significantly increased in the GIII tumors compared with the normal tissue, GI, and GII tumors (Fig. 7; A). Although no significant difference was detected between normal tissues, GI and GII tumors, the expression trend was increasing among the three groups. The average miR-7 expression in the four groups was − 0.013 in the normal tissue, 0.741 in the GI, 2.510 in the GII, and 5.973 in the GIII tumor. The significance coefficient (P value) between GIII tumor and normal tissue, GI and GII tumors was 0.00, 0.02,

and 0.05 respectively (Fig. 6; A). The value of miR-17 expression was 0.00 in the normal tissue, 0.554 in the GI tumor, 0.604 in the GII, and 4.033 in the GIII tumor. The P values between GIII tumor and normal tissue, GI, and GII tumors were 0.00, 0.026, and 0.03 respectively (Fig. 6; A). In addition, the miR-155 expression in normal tissue was 0.005, in the GI tumor was 1.195, in the GII tumor was 1.556, and in the GIII tumor was 4.663. The significance coefficient between GIII tumor and normal tissue, GI, and GII tumors were 0.00, 0.019, and 0.05 respectively (Fig. 6; A). There was no significant difference in the miR-26a expression among the four groups (Fig. 6; A). However, compared with normal tissues, the expression tended to decrease with increasing the tumor grade (Fig. 6; A).

Using the miRWalk database, 1219 mRNAs were detected complementary to the hsa-miR-7-5p 3'-UTR region (score ≤ 95), 4762 mRNAs to the hsa-miR-17-5p 3'-UTR region (score ≤ 95), and 946 mRNAs to the hsa-miR-155-5p 3'-UTR region (score ≤ 95) were detected. By the PPI analysis of these mRNA set interactions, the intersection part of this network was found to consist of 15 mRNAs, including ITPK1, NKAIN3, MKLN1, NF1, TMOD2, SMAD2, EGFR, PIP5K2, RAP1GDS1, ASPH, CACNB4, BACE1, DCP2, CDC42SE2, and APBA1 (Fig. 6; C). The PPI analysis of this cluster (cluster I) identified a network consisting of the EGFR/SMAD1/NF1/BACE1/APBA1 interaction. The EGFR (degree = 3) and ABACE1 (degree = 2) were the mRNAs that must necessarily interact in this PPI network (Fig. 6; D). 143 common mRNAs were detected between the mir-7 and mi17 target mRNAs (Fig. 6; C). The PPI analysis of the cluster (cluster II) revealed a network with 46 nodes and 56 edges. AGO1 and SP1 were the most numerous interacting mRNAs with grade 4. SIRT1 (degree = 7), QK1 (degree = 6), and ATXN1 (degree = 5) were the other core mRNAs in the network of the cluster II PPI (Fig. 6; D). Cluster III, the common mRNAs between miR-17 and miR-155, contained 123 genes (Fig. 6; C). The interaction network of this cluster included 72 nodes and 73 edges. PRKACB and VAPA, with degree 6, were the hub mRNAs in this PPI network. TRPV1 with 5 interactions; then DPYSL3, SCN1A, KCNQ2, USP9X, STX2, and UBE3A with 4 edges were the other most active mRNAs (Fig. 6; D). The cluster IV, which consisted of 26 shared mRNAs from miR-17 and miR-155, did not have a significant interaction network (Fig. 6; C).

Discussion

Although the process of tumor upgrading and the formation of high-grade stem tumor cells is a pathogenic mechanism, using developmental biology perspective may provide a relevant model for this process. In this context, obtaining potential biomarkers to detect the feature of tumor stemness and/or decreasing tumor grade through targeting the markers is essential. The microRNAs with their potential to modulate various signaling pathways are one of the most valuable prospects. In this study, we investigated a potential miRNA cluster actives in high-grade breast stem tumors by promoting the development process of MG.

The enrichment analysis using KEGG pathway terms in grade-specific upregulated DEGs revealed that various mechanisms are active between the undifferentiated and well-differentiated BC (Fig. 2, C-D). Basal transcription factor and MAPK signaling pathway in the GI tumor are mainly activated, while apoptosis mechanism was the remarkable deactivated in these tumors. In GIII tumor, cascades related to

the immune system, including primary immunodeficiency and T- helper (Th) cell development, are strongly involved. On the other hand, several mechanisms of interest, mainly TGF-β and Hippo signaling pathways, were dramatically suppressed in these tumors (Fig. 2; D). Our in silico observation of upregulated DEGs showed that the stage of puberty and pregnancy and lactation were significantly active in the GI and GII breast tumors (Fig. 3; A and B). In contrast, this analysis could not indicate an active MDG mechanism in the GIII BC. Overrepresentation analysis with KEGG pathway collection on the DEGs had relatively conflicting results on DEGs KEGG enrichment. In the GI tumor, ECM-receptor interaction and focal adhesion are the remarkably specific upregulated cascades, while Hippo and TGF-β significantly downregulated (Fig. 4; C). In the GII tumor, ErbB signaling pathways were the interesting upregulated mechanisms along with thyroxine hormone and WNT signaling pathways. The Hippo and ErbB signaling pathways were significantly downregulated (Fig. 4; D). Finally, we observed ErbB, FoxO, and TGFβ were upregulated in the high-grade breast tumor, whereas ECM-receptor interaction, pluripotent stem cell, and PI3K-AKT were the notable downregulated cascades in this tumor (Fig. 4; D). Based on miRNA-mRNA interaction analysis, we found 11 candidate miRNAs in breast tumors with a grade-dependent expression function (Fig. 5; A and B). As exciting mechanisms, the TGF-β, ErbB, RAS, and MAPK signaling pathways were significantly associated with candidate miRNAs, in addition to the EGF receptor (EGFR) tyrosine kinase inhibitor resistance (Fig. 5; C). Our qRT-PCR results on the target miRNAs (miR-7, miR-17, miR-26a, and miR-155) revealed that the expression of the three miRs 7/17/155 was significantly increased in GIII BC compared with the normal tissues and GI/GII tumors (Fig. 7; A). Our PPI network analysis of the three miRs-targeted mRNAs showed that the EGFR was the leading factor active in their intersection PPI network (Fig. 7; C and D).

Butner et al. (2022) demonstrated tumor cell dedifferentiation as a mediator for BC stem cell maintenance [17]. They recognized that the mechanism of dedifferentiation process generation of multipotent cell lineages in the BCs. This multipotent stem cell population of mammary carcinoma is a critical factor for the disease progression and response to therapy [17]. It has been observed that the population of the tumor undifferentiated stem phenotype is significantly higher in high-grade BCs [18]. Considering the stem nature of the high-grade tumors, not obtaining the adult stages of the MGD would be justified. Our in silico analysis of the microarray results shows that by increasing breast tumor stemness (tumor upgrading), activation of the MGD genes decreases according to a definable pattern. The developmental stages of puberty and adult (pregnancy and lactation) are the most involved mechanisms at the lower BC grades. Meanwhile, MG epithelial cell development and differentiation are incredibly active even in well-differentiated tumors.

The EMT is a complex biological process promoted by a series of cascades in the breast tumor cells. These cascades ultimately target the integrity of the extracellular matrix components of the tumor and lead to a change in the character of the well-differentiated BCCs [10, 11, 18]. The TGF-β, WNT, and EGF are the major triggers of the EMT in the most solid malignancies. The TGF-β suppresses E-cadherin biogenesis via the two individual cascades Notch/NF-kB and SMAD4/betta-catenin. The WNT pathway also targets the E-cadherin by triggering Disheveled (Dsh) and betta-catenin in the mammary tumors [19]. Stimulation of the EGFR leads to activation of signal transducer and STAT3 on the BCCs. The STAT3

through transcription factors slug (SNAI) affects the E-cadherin expression and induces the EMT [20]. On the other hand, types of pro-inflammatory cytokines, including interferon-gamma (IFN-γ), interleukin-6 (IL -6), IL -8, and tumor necrosis factor-alpha (TNF-α) are involved in the tumor EMT [21]. These cytokines, via activation of NF-kB signaling, influence this transformation in the MG carcinoma cells [21]. All of the above mechanisms were observed in the BC EMT process. Therefore, one of the fundamental points is which mechanisms regulate EMT in each grade of mammary tumors. Our KEGG enrichment analysis of the grade-specific DEGs did not find significant active EMT mediators in the GI and GII tumors. In contrast, in the GIII tumors, the inflammatory mechanisms and NF-kB were the numerous active signaling pathways in the undifferentiated breast tumors. In contrast, TGF-betta and Notch signaling pathways appeared to be deactivated (Fig. 2). This finding may suggest that immune system activity, both innate and adaptive, is the leading GIII tumor-specific EMT promoter. It shows that targeting the inflammatory response could be an efficient approach to inhibit EMT and improve therapeutic responses in the cases with high-grade BC. However, it can be suggested that as regards the result of EMT is the development of mesenchymal stem cells phenotype [18], justification of cellular heterogeneity of the undifferentiated breast tumor is impossible using the EMT theory.

Due to wild-type regulatory potential, miRNAs have a special position in the diagnosis and treatment of malignancies. Therefore, the exploration of novel miRNAs or miRNA clusters active in the tumor biological functions may pave the way for the development of novel medications. Up to now, some specific miRNAs for the breast stem tumors have been detected [22]. Plummer. et al. (2013) discovered that miR-10b and miR-296b are overexpressed in the high-grade BC and play a significant role in the undifferentiated mammary tumor angiogenesis through stimulation of VEGF expression. By blocking the activity of miR-10b and miR-296b in the experimental models, significant inhibition of the tumor growth was observed [23]. Their results may suggest that the miR-10b and miR-296b make a fortunate miRNA cluster for the targeted therapy of high-grade breast stem tumors. In 2014, Li et al. also found that downregulation of miR-140 in the well-differentiated breast cancer is a critical mechanism for breast cancer stem cell development. Their molecular observation revealed that flowing the miR-140 inhibition, sRY- box transcription factor 9 (SOX9) and aldehyde dehydrogenase 1 (ALDH1) activity promote carcinoma cell dedifferentiation [24]. Their observation could present a sample of how the regulation of miRNA expression could control BC stem cell formation. Loss-of-function of miR-145, miR-200a, and miR-205 has also been demonstrated in the undifferentiated BC flowing the other studies [25–27]. Using the MGD mechanism to detect the grade-specific miRNA-mRNA interaction network in the BC, we show that 11 miRNAs could be candidates for finding a "breast tumor stemness miRNA cluster." By the enrichment analysis with KEGG pathway elevating these 11 miRNAs, we found significant affinity between this miRNA group and the EMT mediators, including the TGF-β signaling, ErbB, as EGFR, signaling pathway, cell adhesion molecules (CAMs), signaling pathways regulating pluripotent stem cells, and also EGRF tyrosine kinase inhibitor resistance (Fig. 5). Our qRT-PCR results show that the expression trend of the three microRNAs 7/17/155 increases with the tumor histological upgrading. This harmonic expression pattern of miR-7, miR-17, and miR-155 indicates that their simultaneous activity may promote the

dedifferentiation of MG carcinoma cells. The ErbB2 and TGF-β signaling pathways were the notable cascades regulated by these three miRNAs (Fig. 7).

The miR-155 is detected as an oncogenic microRNA (oncomiR) in the BC [28]. Previous studies have demonstrated the crucial role of miR-155 in immune cell development [29] and regulation of inflammation in various diseases [30, 31]. It has been reported that the miR-155 is overexpressed in mammary gland tumors. In 2010, Jiang et al. reported that the miR-155 develops carcinogenesis in the MG by inhibiting the tumor suppressor gene suppressor of cytokine signaling 1 (socs1) [28]. They found that the miR-155 induces its oncogenic function via activation of Janus-activated kinase (JAK)/ STAT3 pathway and stimulates proinflammatory cytokines FN -γ and IL -6 on the BCCs [28]. In addition, the miR-155 was found to control the BCC function via the "PIK3R1-FOXO3a-cMYC axis" [32] and downregulation of cell adhesion molecule 1 (CADM1) [33]. The miR-155 regulated cascades are even involved in the dedifferentiation of BCCs. Zuo et al. (2018) found that the level of BC $ABCG2^{+}/CD44^{+}/CD90^{+}$ stem cells were reduced by the miR-155 deactivation in a study using the DA-MB -231 $^{miR155\ -/-}$ cell line [34]. In addition to miR-155, the miR-17 is also considered to be an oncomiR in the BC [35]. The cell cycle regulatory role of this miRNA in normal cells was reported by Cloonan et al. (2008). They investigated that the miR-17-5p controls transition into the G1/S phase of the cell cycle by regulating mitogen-activated protein kinase (MAPK) expression [36]. This miRNA mainly induces migration and invasion in the BCCs via suppressing HMG box-containing protein 1 (HBP1) gene [37]. The HBP1 is a DNA-binding transcription factor leading to the development of amorphous malignant phenotypes [38]. According to the "results from the Norwegian Women and Cancer (NOWAC) study," the expression level of the miR-17-5p was significantly higher in the undifferentiated breast tumors. However, this project discovered that the level of miR-17-5p was significantly decreased in luminal A tumors [39]. This observation may highlight the possible key role of miR-17 in the BC cell dedifferentiation and carcinoma development in the MG. The miR-7 is the other detected oncomiR with a different biological performance than the miRs 17 and 155. It was observed that the miR-7 suppresses BC cell proliferation and viability by activating proteasome activator subunit 3 (REGγ or PSME3) [40]. The PSME3 is critical for breast cancer cell dedifferentiation and induction of EMT [41]. Overexpression of PSME3 in malignant mammary gland cells MDA-MB -231 leads to an increase in the rate of EMT and the development of cancer stem cells [41]. Although miR-7 can promote the formation of undifferentiated cells in breast tumor, Li et al. (2020) discovered that miR-7 reduced the metastatic potential of breast cancer stem cells [42]. Using the MGD mechanism consistent with the above findings, miRNAs 7/17/155 may be a potential breast tumor stem cell miRNA cluster. The results of our in-slice and qRT-PCR demonstrated that the activity level of all three miRs was significantly increased in the undifferentiated breast tumors compared with the lower BC grades and normal tissue groups (Fig. 5–7). The authors believe that the interaction of these three microRNAs through processing a series of MGD mechanisms likely initiates the formation of undifferentiated stem phenotypes in the MG tumors.

The PPI analysis of the intersection of mRNAs shows that the EGFR/NF1/SMAD1/BACE1-related cascades are the most important networks regulated by miRNA cluster 7/17/155 (Fig. 7). The prominent

role of the EGFR in the BCCs EMT has been demonstrated by several observations [10, 11]. The NF1 (Neurofibromin 1) is a GTPase-activating protein. This protein was discovered as a critical Rat sarcoma (RAS)/MAPK pathway inhibitor [43]. The Ras/MAPK signaling pathway, which was also significantly tracked in our GSA analysis, is one of the central targets of EGFR in the dedifferentiation of BC cells [44]. Therefore, the mutation in the NF1 genes is considered one of the critical factors in the formation and development of invasive BC [45]. The SMAD1 (SMAD Family Member 1) is the main downstream of TGF-β and BMPs [46]. It has been reported that the activation of BMP signaling in well-differentiated BC by the SMAD1 promotes cellular dedifferentiation and mammary tumor stemness development [46]. The BACE1 (Beta-secretase 1) is an enzyme that is most active in the formation of β-amyloid [47]. Little is known about the role of this enzyme in the BC biology; it was discovered that the BACE1 is markedly downregulated in the undifferentiated mammary tumors [48]. According to this delivered information, it is arguable that the intersection PPI network of the miRNA 7/17/155 cluster is involved in the development of stem tumors.

Conclusions

By the inspiring MGD mechanism, we discovered specific miRNA-mRNA interaction developmental networks active in each grade of the BC. Our experiment also detected three microRNAs (mir-7, miR-17, and miR-155) as a novel and potential breast tumor stemness miRNA cluster. Using this research strategy, we could present the molecular mechanisms involved in the organ or cell development as an efficient model for finding the tumor development process. From the authors' point of view, the achievements of this study would be used in order: I) the molecular classification of breast cancer, II) the accurate determination of the breast tumor stemness for personalized medicine targets and treatment design, and III) the development of gene or targeted therapy platforms for tumor differentiation therapy. This study also had some limitations that were necessary to accurately prove our theory. Analysis of the expression pattern of this miRNA cluster in a larger statistical population can confirm the accuracy of our results with greater confidence. Moreover, the function of this miRNA cluster in the development of undifferentiated mammary tumors should be confirmed by simultaneously blocking miRNAs 7/17/155 in the high-grade BCCs or experimental models.

Abbreviations

AKT
protein kinase B
APBA1
amyloid beta precursor protein binding family A member 1
ASPH
aspartate beta-hydroxylase
BACE1
beta-secretase 1

BC
breast carcinoma
BCCs
breast cancer cells
BMPs
bone morphogenetic proteins
CACNB4
calcium voltage-gated channel auxiliary subunit beta 4
CAMs
cell adhesion molecules
CDC42SE2
CDC42 small effector 2
DCP2
decapping MRNA 2
DEGs
differential gene expression
DEMs
differential miRNA expression
EGF
epidermal growth factor
EGF
epidermal growth factor
EMT
epithelial to mesenchymal transition
ErbB
epidermal growth factor receptor
FGF
fibroblast growth factor
FoxO
forkhead box transcription factors
GATA3
GATA binding protein 3
GEO
gene expression omnibus database
GO
gene ontology
IFN-γ
including interferon-gamma
IGF 1/2
insulin-like growth factor 1/2

IL
interleukin
TNFα
tumor necrosis factor-alpha
ITPK1
inositol 1,3,4-triphosphate 5/6 kinase
MAPK
mitogen-activated protein kinase
MG
Mammary glands
MGD
mammary gland development
miR
microRNA
MKLN1
muskelin1
NF1
Neurofibromatosis type1
NKAIN3
sodium/potassium transporting ATPase interacting 3
PI3K
phosphatidylinositol 3-kinase
PIP5K2
arabidopsis phosphatidylinositol 4-phosphate 5-kinase 2
PPI
protein-protein interaction
RAP1GDS1
rap1 GTPase-GDP dissociation stimulator1
RAS
rat sarcoma
SMAD2
mothers against decapentaplegic homolog 2
STAT
signal transducer and activator of transcription
TGFβ
transforming growth factorβ
TMOD2
tropomodulin2
VEGF
vascular endothelial growth factor

WNT
wingless-related integration site

Declarations

Acknowledgements

Non

Authors’ contributions

SKh and HKh: project management, conceptualization, data curation, analysis, software, visualisation, carry out genetic tests, and original draft preparation. HJ, HM and MD: review, editing, and supervision. ES and AF: data analysis, software, visualisation, and original draft preparation. MY and RSh: bioinformatic and genomic analysis, manuscript review, and editing. AM and AE-R: tissue preparation and pathological procedure. FH, RO, and KN: review and editing

Funding

This work was supported by the Tehran University of Medical Sciences (Projects Code: 1400-2-259-54530).

Availability of data and materials

All data generated or analyzed during this study are available.

Ethics approval and consent to participate

This study was approved by the Research Ethics Committees of Imam Khomeini Hospital Complex-Tehran University of Medical Sciences (NO: IR.TUMS.IKHC.REC.1400.506).

Consent for publication

Non

Author details

1- Breast Disease Research Center, Tehran University of Medical Sciences, Tehran, Iran.2- Department of Animal Biology, Faculty of Biological Sciences, Kharazmi University, Tehran, Iran. 3- Department of Stem Cells and Developmental Biology, Cell Science Research Center, Royan Institute for Stem Cell Biology and Technology, ACECR, Tehran, Iran. 4- Biostatistics group, Department of Health Sciences, University of Leicester, UK. 5- Cancer Biology Research Center, Cancer Research Institute, Imam Khomeini Hospital Complex, Tehran University of Medical Sciences, Tehran, Iran. 6- Iran National Tumor Bank, Cancer Institute of Iran, Tehran University of Medical Sciences, Tehran. 7- Students' Scientific Research Center

(SSRC), Tehran University of Medical Sciences, Tehran, Iran 8- International Center for Personalized Medicine (ICPM-P7MEDICINE), Düsseldorf, Germany

References

1. Slepicka PF, Somasundara AVH, Dos Santos CO: **The molecular basis of mammary gland development and epithelial differentiation.** In *Seminars in Cell & Developmental Biology*. Elsevier; 2021: 93-112.
2. Dawson CA, Visvader JE: **The cellular organization of the mammary gland: insights from microscopy.** *Journal of Mammary Gland Biology and Neoplasia* 2021, **26:**71-85.
3. Watson CJ, Khaled WT: **Mammary development in the embryo and adult: a journey of morphogenesis and commitment.** 2008.
4. Fu NY, Nolan E, Lindeman GJ, Visvader JE: **Stem cells and the differentiation hierarchy in mammary gland development.** *Physiological reviews* 2020, **100:**489-523.
5. Khodayari H, Khodayari S, Khalighfard S, Tahmasebifar A, Tajaldini M, Poorkhani A, Nikoueinejad H, Hamidi GA, Nosrati H, Kalhori MR: **Gamma-radiated immunosuppressed tumor xenograft mice can be a new ideal model in cancer research.** *Scientific Reports* 2021, **11:**1-13.
6. Farhanji B, Latifpour M, Alizadeh AM, Khodayari H, Khodayari S, Khaniki M, Ghasempour S: **Tumor suppression effects of myoepithelial cells on mice breast cancer.** *European journal of pharmacology* 2015, **765:**171-178.
7. Wang Y, Liao R, Chen X, Ying X, Chen G, Li M, Dong C: **Twist-mediated PAR1 induction is required for breast cancer progression and metastasis by inhibiting Hippo pathway.** *Cell death & disease* 2020, **11:**1-12.
8. Adorno-Cruz V, Hoffmann AD, Liu X, Dashzeveg NK, Taftaf R, Wray B, Keri RA, Liu H: **ITGA2 promotes expression of ACLY and CCND1 in enhancing breast cancer stemness and metastasis.** *Genes & diseases* 2021, **8:**493-508.
9. Barua A, Choudhury P, Mandal S, Panda CK, Saha P: **Anti-metastatic potential of a novel xanthone sourced by Swertia chirata against in vivo and in vitro breast adenocarcinoma frameworks.** *Asian Pacific Journal of Cancer Prevention: APJCP* 2020, **21:**2865.
10. Wendt MK, Smith JA, Schiemann WP: **Transforming growth factor-β-induced epithelial–mesenchymal transition facilitates epidermal growth factor-dependent breast cancer progression.** *Oncogene* 2010, **29:**6485-6498.
11. Pasquier J, Abu-Kaoud N, Al Thani H, Rafii A: **Epithelial to mesenchymal transition in a clinical perspective.** *Journal of oncology* 2015, **2015**.
12. Isanejad A, Alizadeh AM, Shalamzari SA, Khodayari H, Khodayari S, Khori V, Khojastehnjad N: **MicroRNA-206, let-7a and microRNA-21 pathways involved in the anti-angiogenesis effects of the interval exercise training and hormone therapy in breast cancer.** *Life sciences* 2016, **151:**30-40.

13. Khori V, Shalamzari SA, Isanejad A, Alizadeh AM, Alizadeh S, Khodayari S, Khodayari H, Shahbazi S, Zahedi A, Sohanaki H: **Effects of exercise training together with tamoxifen in reducing mammary tumor burden in mice: possible underlying pathway of miR-21.** *European journal of pharmacology* 2015, **765:**179-187.
14. Wang J, Hao Z, Hu J, Liu X, Li S, Wang J, Shen J, Song Y, Ke N, Luo Y: **Small RNA deep sequencing reveals the expressions of microRNAs in ovine mammary gland development at peak-lactation and during the non-lactating period.** *Genomics* 2021, **113:**637-646.
15. Jiang N, Wu C, Li Y, Liu J, Yuan Y, Shi H: **Identification and profiling of microRNAs involved in the regenerative involution of mammary gland.** *Genomics* 2022, **114:**110442.
16. Damavandi Z, Torkashvand S, Vasei M, Soltani BM, Tavallaei M, Mowla SJ: **Aberrant expression of breast development-related microRNAs, miR-22, miR-132, and miR-212, in breast tumor tissues.** *Journal of Breast Cancer* 2016, **19:**148-155.
17. Butner JD, Dogra P, Chung C, Ruiz-Ramírez J, Nizzero S, Plodinec M, Li X, Pan P-Y, Chen S-h, Cristini V: **Dedifferentiation-mediated stem cell niche maintenance in early-stage ductal carcinoma in situ progression: insights from a multiscale modeling study.** *Cell death & disease* 2022, **13:**1-10.
18. Tisza MJ, Zhao W, Fuentes JS, Prijic S, Chen X, Levental I, Chang JT: **Motility and stem cell properties induced by the epithelial-mesenchymal transition require destabilization of lipid rafts.** *Oncotarget* 2016, **7:**51553.
19. Foroni C, Broggini M, Generali D, Damia G: **Epithelial–mesenchymal transition and breast cancer: Role, molecular mechanisms and clinical impact.** *Cancer treatment reviews* 2012, **38:**689-697.
20. Wang T, Yuan J, Zhang J, Tian R, Ji W, Zhou Y, Yang Y, Song W, Zhang F, Niu R: **Anxa2 binds to STAT3 and promotes epithelial to mesenchymal transition in breast cancer cells.** *Oncotarget* 2015, **6:**30975.
21. Suarez-Carmona M, Lesage J, Cataldo D, Gilles C: **EMT and inflammation: inseparable actors of cancer progression.** *Molecular oncology* 2017, **11:**805-823.
22. Humphries B, Wang Z, Yang C: **MicroRNA Regulation of Breast Cancer Stemness.** *International Journal of Molecular Sciences* 2021, **22:**3756.
23. Plummer PN, Freeman R, Taft RJ, Vider J, Sax M, Umer BA, Gao D, Johns C, Mattick JS, Wilton SD: **MicroRNAs Regulate Tumor Angiogenesis Modulated by Endothelial Progenitor CellsmiRNA Regulation of Bone Marrow–Mediated Tumor Angiogenesis.** *Cancer research* 2013, **73:**341-352.
24. Li Q, Yao Y, Eades G, Liu Z, Zhang Y, Zhou Q: **Downregulation of miR-140 promotes cancer stem cell formation in basal-like early stage breast cancer.** *Oncogene* 2014, **33:**2589-2600.
25. Götte M, Mohr C, Koo C, Stock C, Vaske A, Viola M, Ibrahim S, Peddibhotla S, Teng YH, Low J: **miR-145-dependent targeting of junctional adhesion molecule A and modulation of fascin expression are associated with reduced breast cancer cell motility and invasiveness.** *Oncogene* 2010, **29:**6569-6580.
26. Stankevicins L, Barat A, Dessen P, Vassetzky Y, de Moura Gallo C: **The microRNA-205-5p is correlated to metastatic potential of 21T series: A breast cancer progression model.** *PLoS One* 2017, **12:**e0173756.

27. Tsai H-P, Huang S-F, Li C-F, Chien H-T, Chen S-C: **Differential microRNA expression in breast cancer with different onset age.** *PLoS One* 2018, **13:**e0191195.
28. Jiang S, Zhang H-W, Lu M-H, He X-H, Li Y, Gu H, Liu M-F, Wang E-D: **MicroRNA-155 functions as an OncomiR in breast cancer by targeting the suppressor of cytokine signaling 1 gene.** *Cancer research* 2010, **70:**3119-3127.
29. Wang J, Li K, Zhang X, Li G, Liu T, Wu X, Brown SL, Zhou L, Mi Q-S: **MicroRNA-155 Controls i NKT Cell Development and Lineage Differentiation by Coordinating Multiple Regulating Pathways.** *Frontiers in cell and developmental biology* 2021, **8:**619220.
30. Dickey LL, Worne CL, Glover JL, Lane TE, O'Connell RM: **MicroRNA-155 enhances T cell trafficking and antiviral effector function in a model of coronavirus-induced neurologic disease.** *Journal of neuroinflammation* 2016, **13:**1-12.
31. Mahesh G, Biswas R: **MicroRNA-155: a master regulator of inflammation.** *Journal of Interferon & Cytokine Research* 2019, **39:**321-330.
32. Kim S, Lee E, Jung J, Lee JW, Kim HJ, Kim J, Lee HJ, Chae SY, Jeon SM, Son BH: **microRNA-155 positively regulates glucose metabolism via PIK3R1-FOXO3a-cMYC axis in breast cancer.** *Oncogene* 2018, **37:**2982-2991.
33. Zhang G, Zhong L, Luo H, Wang S: **MicroRNA-155-3p promotes breast cancer progression through down-regulating CADM1.** *OncoTargets and therapy* 2019, **12:**7993.
34. Zuo J, Yu Y, Zhu M, Jing W, Yu M, Chai H, Liang C, Tu J: **Inhibition of miR-155, a therapeutic target for breast cancer, prevented in cancer stem cell formation.** *Cancer Biomarkers* 2018, **21:**383-392.
35. Hossain A, Kuo MT, Saunders GF: **Mir-17-5p regulates breast cancer cell proliferation by inhibiting translation of AIB1 mRNA.** *Molecular and cellular biology* 2006, **26:**8191-8201.
36. Cloonan N, Brown MK, Steptoe AL, Wani S, Chan WL, Forrest AR, Kolle G, Gabrielli B, Grimmond SM: **The miR-17-5p microRNA is a key regulator of the G1/S phase cell cycle transition.** *Genome biology* 2008, **9:**1-14.
37. Li H, Bian C, Liao L, Li J, Zhao RC: **miR-17-5p promotes human breast cancer cell migration and invasion through suppression of HBP1.** *Breast cancer research and treatment* 2011, **126:**565-575.
38. Yu S, Yang D, Ye Y, Liu P, Chen Z, Lei T, Pu J, Liu L, Wang Z: **lncRNA AFAP1-AS1 promotes malignant phenotype through binding with LSD1 and repressing HBP1 in non-small cell lung cancer.** *Cancer Sci* 2019, **110:**2211-2225.
39. Moi L, Braaten T, Al-Shibli K, Lund E, Busund L-TR: **Differential expression of the miR-17-92 cluster and miR-17 family in breast cancer according to tumor type; results from the Norwegian Women and Cancer (NOWAC) study.** *Journal of translational medicine* 2019, **17:**1-20.
40. Shi Y, Luo X, Li P, Tan J, Wang X, Xiang T, Ren G: **miR-7-5p suppresses cell proliferation and induces apoptosis of breast cancer cells mainly by targeting REGγ.** *Cancer letters* 2015, **358:**27-36.
41. Yi Z, Yang D, Liao X, Guo F, Wang Y, Wang X: **PSME3 induces epithelial–mesenchymal transition with inducing the expression of CSC markers and immunosuppression in breast cancer.** *Experimental Cell Research* 2017, **358:**87-93.

42. Li M, Pan M, Wang J, You C, Zhao F, Zheng D, Guo M, Xu H, Wu D, Wang L: **miR-7 reduces breast cancer stem cell metastasis via inhibiting RELA to decrease ESAM expression.** *Molecular Therapy-Oncolytics* 2020, **18:**70-82.
43. Peltonen S, Kallionpää RA, Peltonen J: **Neurofibromatosis type 1 (NF1) gene: Beyond café au lait spots and dermal neurofibromas.** *Experimental Dermatology* 2017, **26:**645-648.
44. Hao P, Huang Y, Peng J, Yu J, Guo X, Bao F, Dian Z, An S, Xu T-R: **IRS4 promotes the progression of non-small cell lung cancer and confers resistance to EGFR-TKI through the activation of PI3K/Akt and Ras-MAPK pathways.** *Experimental Cell Research* 2021, **403:**112615.
45. Tao J, Sun D, Dong L, Zhu H, Hou H: **Advancement in research and therapy of NF1 mutant malignant tumors.** *Cancer cell international* 2020, **20:**1-8.
46. Serrao A, Jenkins LM, Chumanevich AA, Horst B, Liang J, Gatza ML, Lee NY, Roninson IB, Broude EV, Mythreye K: **Mediator kinase CDK8/CDK19 drives YAP1-dependent BMP4-induced EMT in cancer.** *Oncogene* 2018, **37:**4792-4808.
47. Taylor HA, Przemylska L, Clavane EM, Meakin PJ: **BACE1: More than just a β-secretase.** *Obesity Reviews* 2022**:**e13430.
48. Yaghoobi H, Azizi H, Banitalebi-Dehkordi M, Rezaei FM, Arsang-Jnag S, Taheri M, Ghafouri-Fard S: **Beta-secretase 1 (BACE1) is down-regulated in invasive ductal carcinoma of breast.** *Reports of Biochemistry & Molecular Biology* 2019, **8:**200.

Tables

Table 1 is available in the Supplementary Files section.

Figures

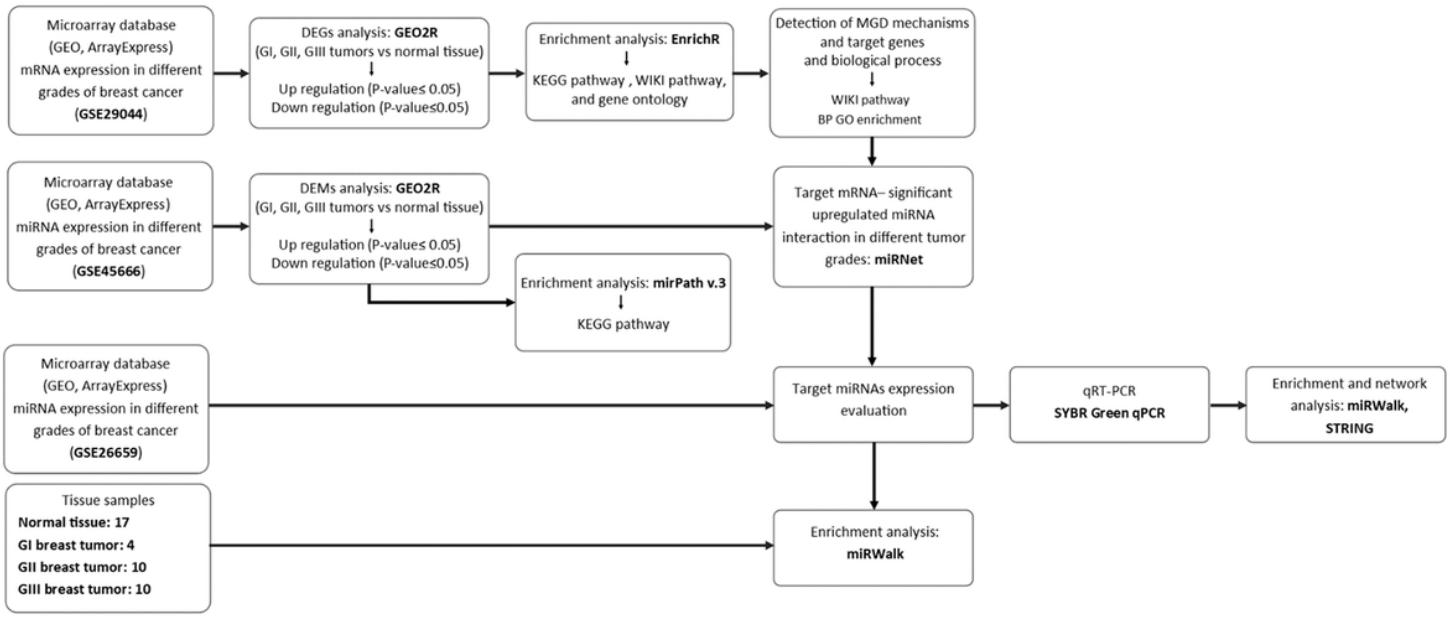

Figure 1

Workflow of the study. The flowchart illustrates the methodology used in the current study.

Figure 2

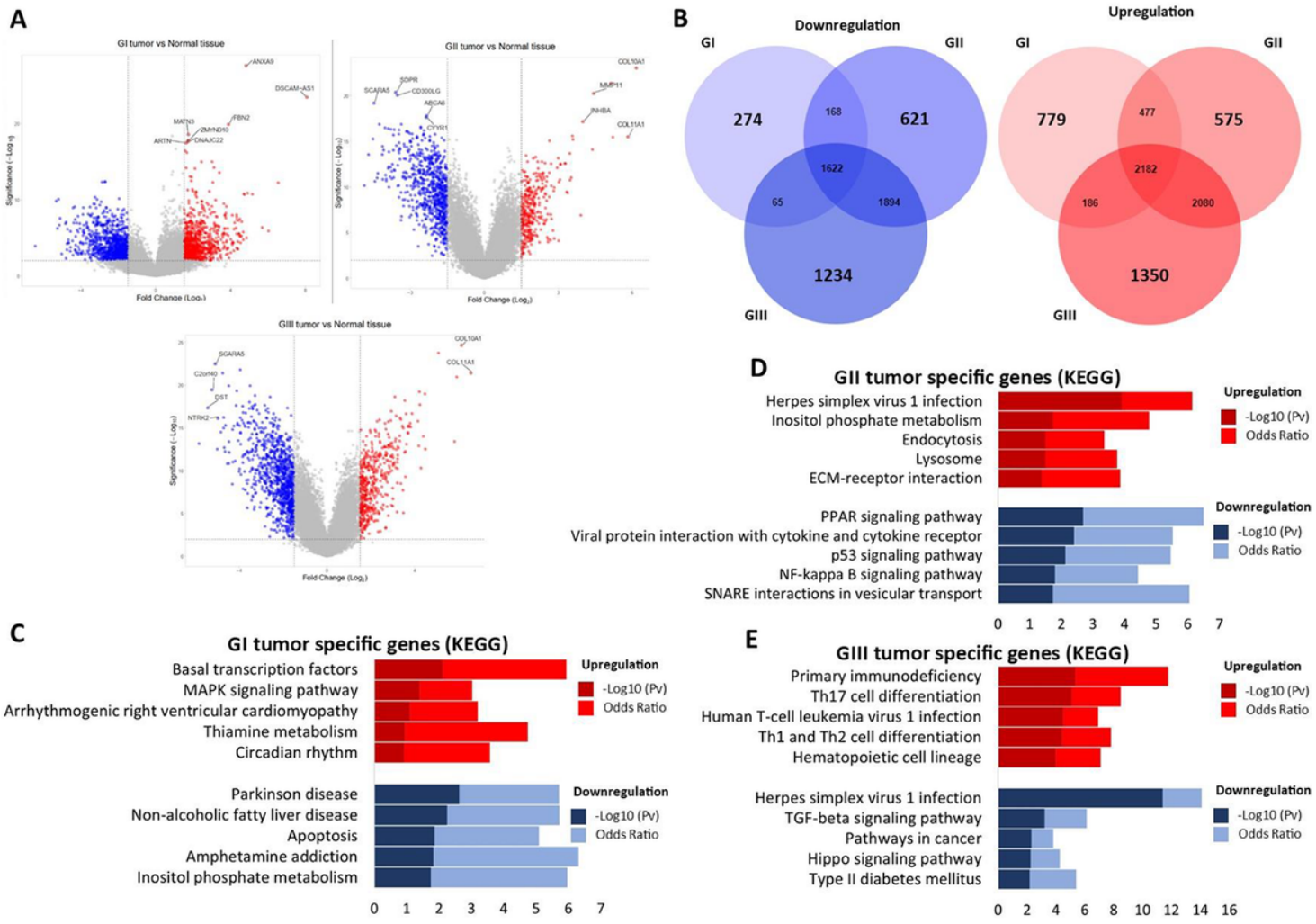

Bioinformatic analysis of GSE29044 data. A) Volcano plots of differential mRNA expression analysis of GI, GII, and GIII breas t tumors compared to normal tissue, B) Venn diagram showing the overlap of upregulated (red diagram) and downregulated (blue diagram) between three BC grades, and C, D, E) KEGG pathway enrichment analysis of upregulated (red diagrams) and downregulated (blue diagrams) mRNA s in three BC grades. Bars show Log10 (P value) and odds

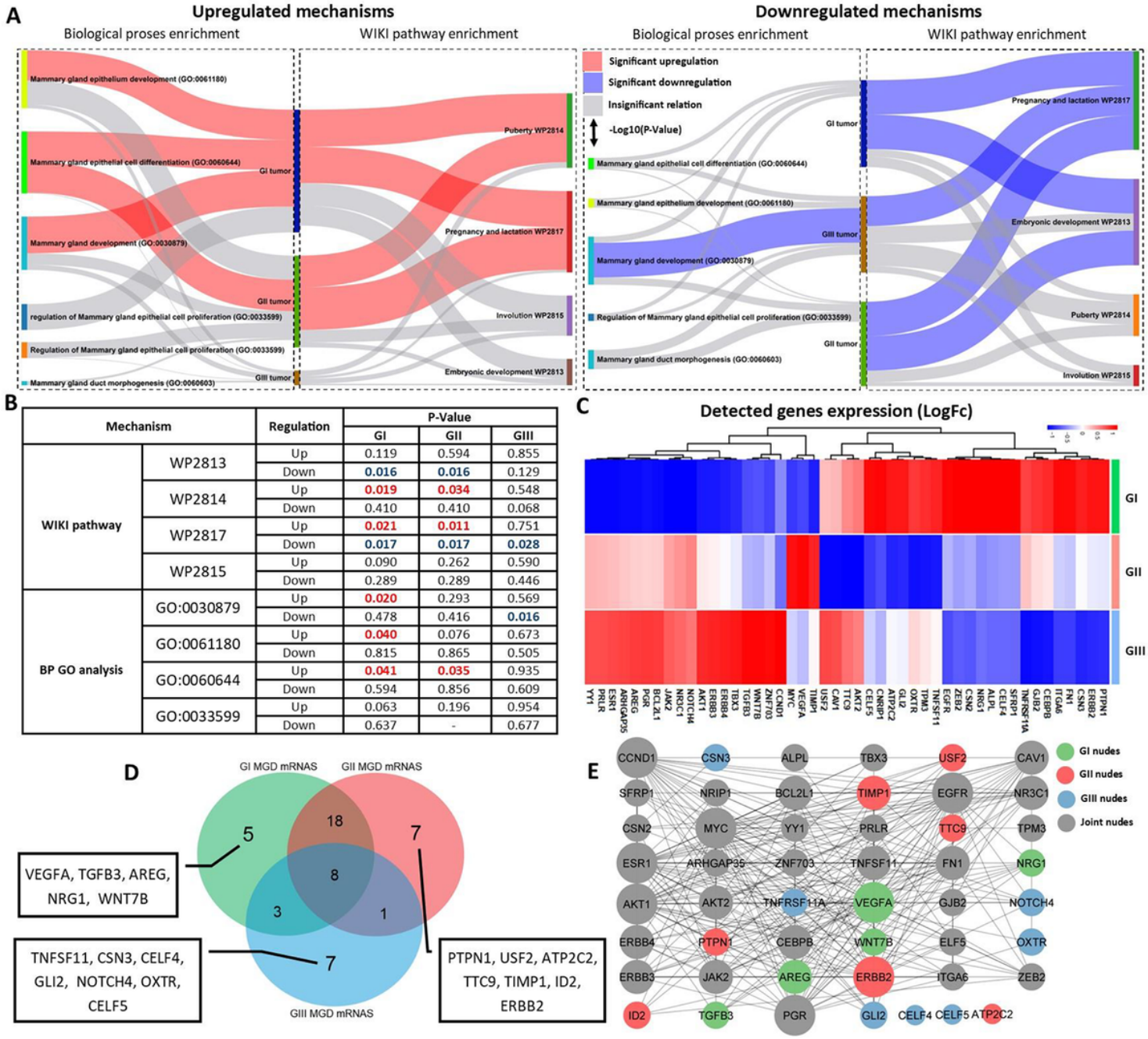

Mechanism		Regulation	P-Value		
			GI	GII	GIII
WIKI pathway	WP2813	Up	0.119	0.594	0.855
		Down	0.016	0.016	0.129
	WP2814	Up	0.019	0.034	0.548
		Down	0.410	0.410	0.068
	WP2817	Up	0.021	0.011	0.751
		Down	0.017	0.017	0.028
	WP2815	Up	0.090	0.262	0.590
		Down	0.289	0.289	0.446
BP GO analysis	GO:0030879	Up	0.020	0.293	0.569
		Down	0.478	0.416	0.016
	GO:0061180	Up	0.040	0.076	0.673
		Down	0.815	0.865	0.505
	GO:0060644	Up	0.041	0.035	0.935
		Down	0.594	0.856	0.609
	GO:0033599	Up	0.063	0.196	0.954
		Down	0.637	-	0.677

Figure 3

M echanisms of mammary gland development in each grade of the BC and expression of detected miRNAs. A) Sankey diagram illustrating the contribution of different MGD stages in GI, GII, and GIII BCs. In both Sankey diagrams, the first (left) and second axes re present the relationship between the biological processes GO enrichment findings and GI, GII, and GIII tumors. The third (right) and second axes also represent the association between WIKI pathway enrichment findings and GI, GII, and GIII tumors. The red g raph refers to upregulated DGEs and the blue graph refers to downregulated DGEs. Red and blue ribbons show a significant correlation, and gray bands indicate insignificant correlation. The width of each reborn shows the Log10(P Value) of the mechanisms. B) Table showing the P value level of detected mechanisms found in each grade of BCs. Numbers highlighted in red refer to significantly up

regulated mechanisms, and numbers highlighted in blue refer to significantly down regulated mechanisms. C: Heatmaps sh owing the expression level of target mRNAs in three different BC grades compared with normal tissue based on LogFc. D) Venn diagram showing the ov erlap of detected MGD mRNAs between the three BC grades. E) PPI interaction of detected MGD mRNAs between thre e BC grades. The size of the nose shows the most interacting mRNAs and the color of the nodes refers to the group of mRNAs.

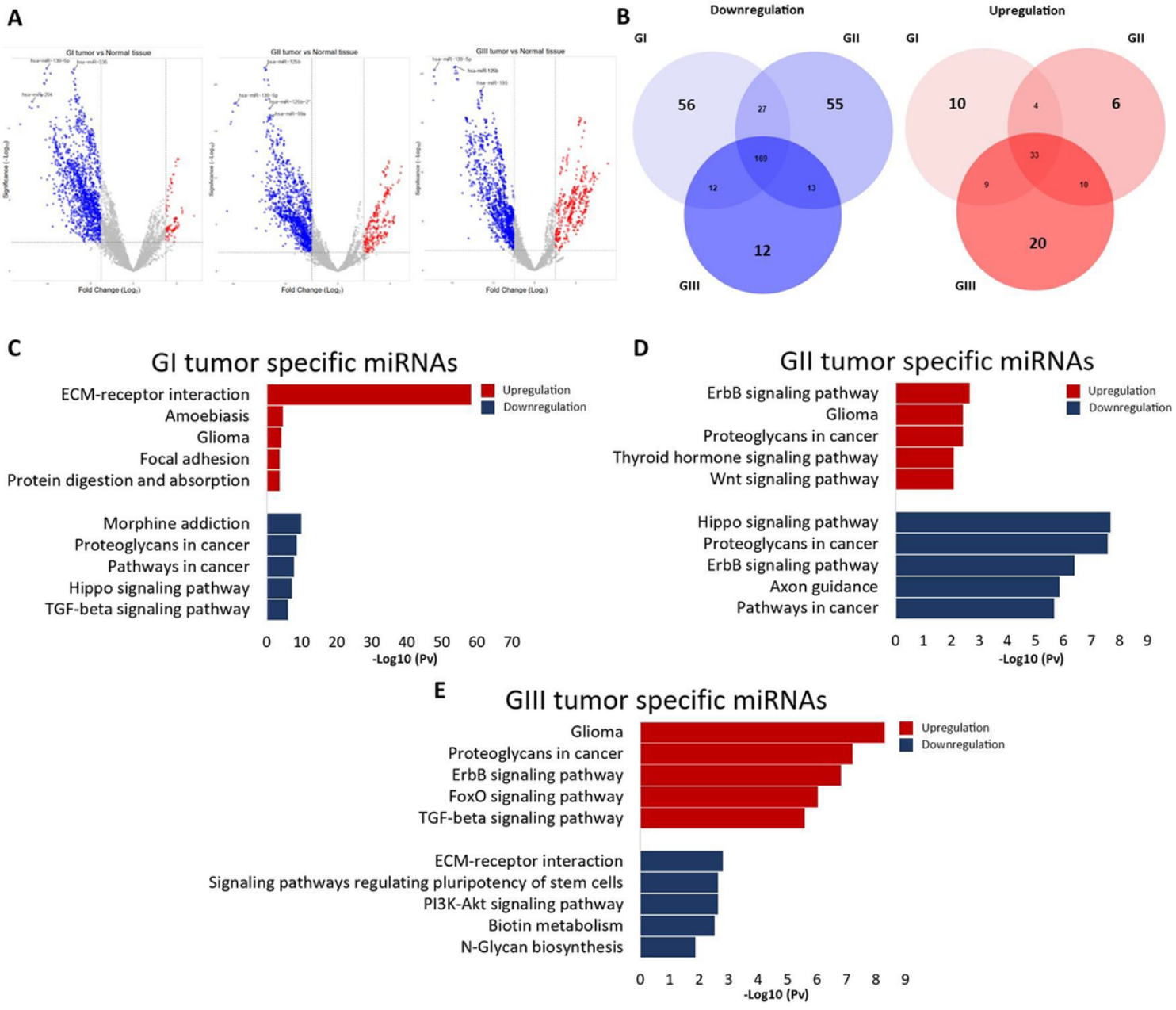

Figure 4

Bioinformatic analysis of GSE45666 data. A) Volcano plots of differential miRNA expression analysis of GI, GII and GIII breast tumors compared to normal tissues, B) Venn diagram showing the overlap of upregulated (red diagram) and downregulated (blue diagram) between three BC grades, and C, D, E) KEGG

pathway enrichment analysis of upregulated (red diagrams) and downregulated (blue diagrams) miRNAs in three BC grades. Bars represent Log10 (P value).

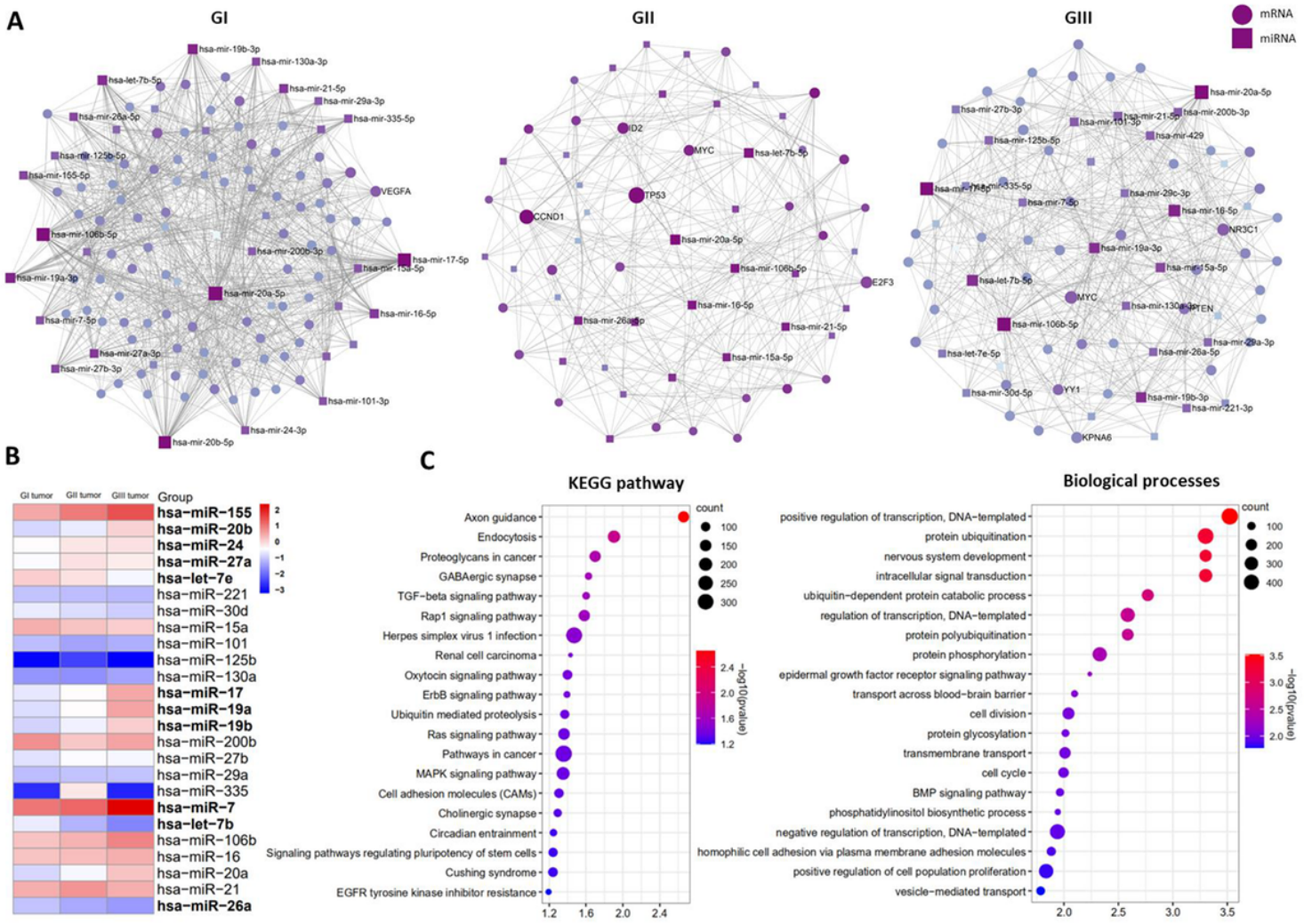

Figure 5

Analysis of miRNA mRNA network and expression pattern of hub miRNAs in different grades of BC. A) miRNA mRNA interaction network in GI, GII, and GIII BCs. The square nodes refer to miRNAs and the circular nodes refer to mRNAs. The node's size and color sha rpness show the most interacting nodes. (B) Heatmaps show the expression level of miRNAs in three different BC grades compare d to normal tissue based on LogFc. Red indicates upregulation, blue indicates downregulation, D) E nrichment analysis with KEGG path way in eleven candidate miRNAs, and E) B iological process enrichment GO in eleven candidate miRNAs.

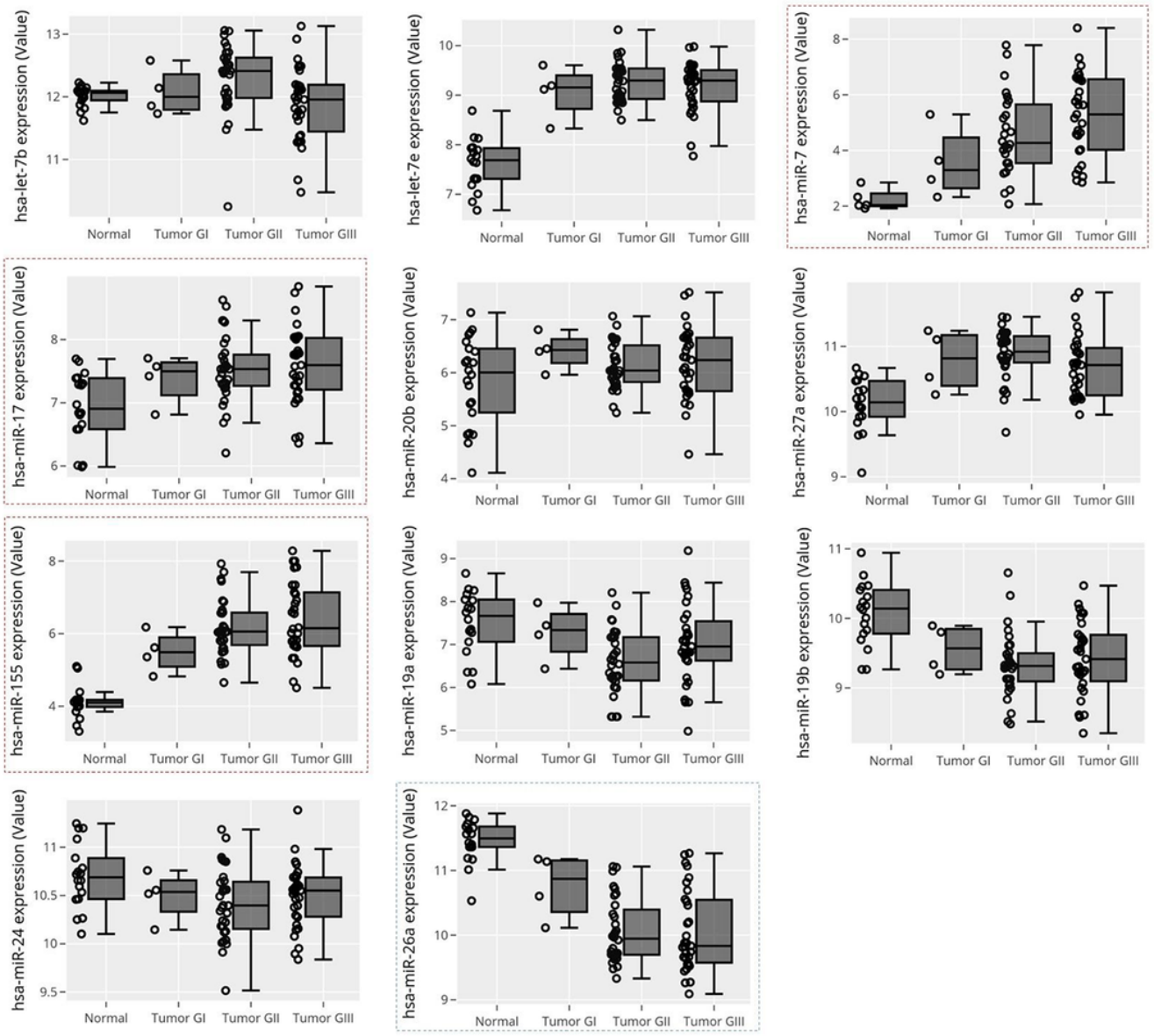

Figure 6

The expression level of the candidate miRNAs in normal tissues and different grades of BCs. The row expression levels (Fc) of the GSE26659 samples were used. Boxes highlighted in red refer to gain of function miRNAs and boxes highlighted in blue refer to loss of function miRNAs. Normalization values are in log2.

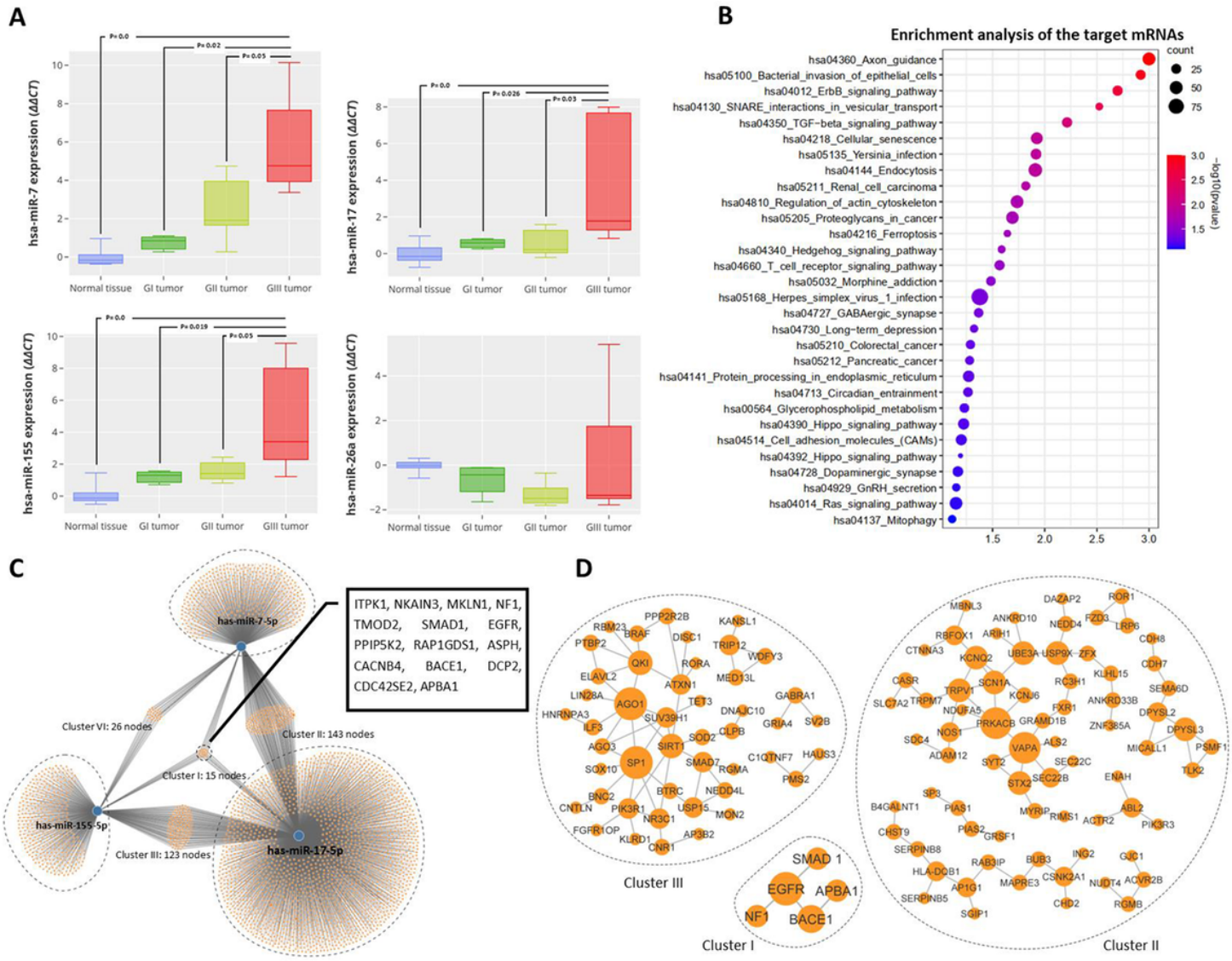

Figure 7

qRT PCR result of the target miRNA and its target miRNAs interaction network. A) Boxplots represent the expression of miR 7, miR 17, miR 26a and miR 155 in normal tissues and GI, GII, and GIII tumors. miRNA expression normalization using the standard compa rative CT (ΔΔCT) method. B) E nrichment analysis with KEGG pathway on miRNAs with significant change in expression. C) Map of interactions between target miRNAs and mRNAs. Cluster I refer to intermediate miRNAs between three miRNAs, cluster II refers to sha red mRNAs between miR 7 and miR 17, cluster II refers to shared mRNAs between miR 17 and miR 155, and cluster VI also refers to shared mRNAs between miR 155 and miR 7. D) Different clusters PPI network. The nodes' size presents the interaction level.

Supplementary Files

This is a list of supplementary files associated with this preprint. Click to download.

- Table1.pdf